

# An on-engine method for dynamic characterisation of $NO_x$ concentration sensors

J. Galindo, J.R. Serrano, C. Guardiola, D.Blanco-Rodriguez

*CMT Motores Térmicos, Universidad Politécnica de Valencia, Camino de Vera s/n, E-46022 Valencia, Spain*

I.G.Cuadrado

*Empresa Integral S.A. Medellin, Colombia*

---

## Abstract

An on-engine method for dynamic characterisation of automotive  $NO_x$  concentration sensors is presented. Steps in start of injection on a diesel engine are employed to achieve step-like  $NO_x$  concentration variations on exhaust flow. On the basis of the sensor response, delay and dynamic response can be easily identified; the paper shows a simple least squares procedure although other models and identification techniques could be used. Application data is presented for three  $NO_x$  sensors: a research-grade chemiluminescence exhaust gas analyser, and two different commercial  $ZrO_2$ -based sensors.

*Keywords:* combustion engine;  $NO_x$ ;  $ZrO_2$  sensor; SOI; measurement techniques; sensor calibration; on-board diagnostics

*PACS:* 5.70.a, 89.40.Bb

---

## 1. Introduction

World attention about environmental protection resulted in new strict laws which establish the requirements for pollutants emissions, and therefore define priorities in the technology development. Particularly in mobile sources, diesel engines must reduce  $NO_x$  emissions by 20% with Euro 5 and 50% with Euro 6, with respect to previous Euro 4 standards[1].

Engine development has to guarantee low emissions while keeping or achieving higher efficiency, performance and reliability. This purpose requires not only efforts on engine design and on operating conditions, but also in the development of reliable measurement systems to get information about the process, which is needed for the implementation of control strategies, specially for transient conditions[2].

Recent improvements in  $NO_x$  sensor technologies and, among them, those which are based on  $ZrO_2$  [3] employed to measure gas at wet condition (i.e. without removing exhaust gas water steam content), allow an on-board measurement of the  $NO_x$  concentration. Closed loop control and on-board diagnosis for nitrogen oxide engine emissions reduction can be based on models[4,

---

*Email addresses:* galindo@mot.upv.es (J. Galindo), jrserran@mot.upv.es (J.R. Serrano), carguaga@mot.upv.es (C. Guardiola), dablarod@mot.upv.es (D.Blanco-Rodriguez)

*Preprint submitted to Experimental Thermal and Fluid Science*

*December 2, 2016*

5], but more commonly are confined to fixed calibrations. Several studies have evaluated the accuracy and time response of real time  $NO_x$  sensor measurements for these applications[6, 7].

$NO_x$  sensors based on planar  $ZrO_2$  technology have suffered a big evolution over the last 15 years[3] and now are manufactured using the planar zirconia multilayer technology[8], which combines thick film screen printing and ceramic tape casting[9]. Last versions of these sensors offer reduced warmup time, smaller size, lower weight and cost-effective production, which encourage their implementation on commercial engines. This kind of sensors simultaneously provides a measurement of the relative air-to-fuel ratio ( $\lambda$ ) and  $NO_x$  concentration:

In a first cavity, an electrochemical pump adjusts the oxygen concentration to a predefined value, thus providing a linear measurement of  $\lambda$ . At the same time, a fast binary output is provided, differentiating between rich and lean conditions in the exhaust gases.

In a second cavity, the oxygen produced through the dissociation of  $NO_x$  is pumped out in a similar way by means of a second electrochemical pump. The output of this pump is proportional to the  $NO_x$  concentration in the exhaust gases.

Such "amperometric  $NO_x$  and oxygen sensing device" could be the key for the selective catalyst reduction (SCR) systems[10] (although improvements in precision as it is mentioned in [11] are needed to fulfil current laws) or for improving exhaust gas recirculation (EGR) control when important cylinder-to-cylinder distribution dispersion appears[12].

Since sensors are subject to unit-to-unit manufacturing discrepancies, and can be affected by significant drift during their lifespan, methods for the online characterisation of sensors would improve the application of these for automotive control purposes. Usual calibration methods consist of a specific test rig which generates known composition synthesis gas which is used for the static and dynamic calibration of the sensor, while high speed valves are needed for dynamic calibration[13], or some solutions based on openly mounted sensors with valves allocated before the sensor, where gas composition is changed within milliseconds[14]. However, these calibration methods are restricted to laboratory use and cannot be performed during the operation phase on the engine.

This paper presents an easy on-engine experiment for  $NO_x$  sensors calibration and dynamic identification. The method uses the internal combustion engine as a gas generator, using modifications in the start of injection (SOI) for generating step-like transients in  $NO_x$  concentration.

In section 2 a short description of the experimental set-up used is presented. On the basis of the experimental tests, it will be shown in section 3 that step variations (of limited size) in SOI cause step-like modifications in  $NO_x$  concentration while maintaining the rest of operative variables almost constant. This fact will be profited for providing data for identifying  $NO_x$  sensor dynamics. An example of identification of a linear first-order model is presented on section 4, with the application to three different sensors. Finally, section 5 discusses the perspective of the on-board application of the method and section 6 presents the conclusions

## 2. Experimental set-up

Test engine was an automotive 2.2-litre 4-cylinder common rail diesel engine. Engine specifications are shown in Table 1; for the experiments, all after-treatment devices were removed. An external calibrable ECU (electronic control unit) allowed varying injection parameters, such as injection pressure, SOI and injection duration, and also boost and EGR control set points. The engine was installed on an engine test bench and coupled to a variable frequency eddy current dynamometer that allowed carrying out dynamical tests. The layout of the experimental set-up is shown in Figure 1.

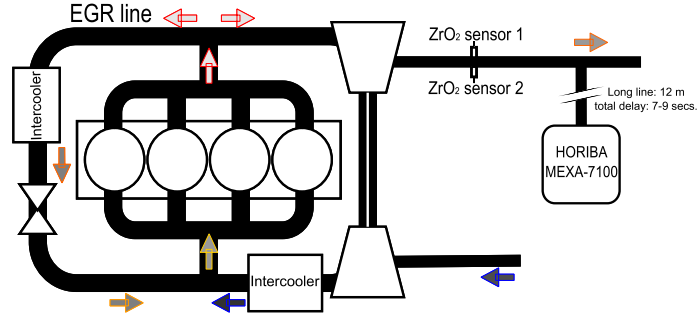


Figure 1: Test bench layout.

Stroke ( $S$ )	96 mm
Bore ( $D$ )	85 mm
$S/D$	1.129
Number of cylinders ( $z$ )	4
Displacement	2179 $cm^3$
Turbocharging system	Sequential parallel[15]
Valves by cylinder	4
Maximum power	125 kW@4000 rpm
Compression ratio	17:1

Table 1: Engine main characteristics.

Horiba MEXA 7100DEGR gas analyser was used as  $NO_x$  calibration standard. This has a measuring range from 0 to 5000 ppm. The gas probe was located at the end of the exhaust line, thus corresponding to engine out emissions.  $NO_x$  were measured on a dry basis, by means of a heated chemiluminescence detector (HCLD) type with a  $NO_2/NO$  converter. Calibration gases were used for the calibration of the system (zero and span).

Three key factors did not allow using this system as dynamic calibration method:

1. Measurement system time response, which includes the signal rising time, is slower than the tested  $ZrO_2$  sensors.
2. A long line is used for providing exhaust gas to the gas analyser (12m). This long line causes not only a transport delay, but also can cause diffusive effects.
3. Soot-free gas is needed in order to prevent sensor damage; therefore a filter is used in the line[16]. In transient engine operation, filter contributes to substantial emission signal distortion.

It is worth noting that some studies combine experimental data and phenomenological modelling approach to synchronise[2, 17] or to restore[18, 19] the signals from slow response analysers during transient engine operation. This is done by analytical means, using simple gas diffusion model and perfect gas mixing models or through a control theory approach to the problem. The correction based on control oriented data-driven models is partially treated in this paper, as

with the proposed method a sensor model can be obtained, which is the first requirement for this kind of approach. However, other approaches appear quite complex and are not undertaken here.

For the present work, two  $NO_x$  sensors from different suppliers, both based in the planar  $ZrO_2$  technology, were selected (hereinafter sensor 1 and sensor 2). Both sensors were located downstream the turbine, upstream the usual location of the after-treatment systems (which, as indicated before, were removed for the tests). Note that  $NO_x$  sensors in current engines are usually located downstream the SCR system and, although some engine models can fit a second sensor upstream the SCR, usually raw  $NO_x$  is estimated through models[10]. Hence, the results shown in the next sections are not directly applicable to the usual sensor location. This issue will be discussed in section 5.

### 3. Methodology

Calibration methodology was based on generating exhaust gases with different  $NO_x$  concentrations by means of the modification of the engine injection settings.

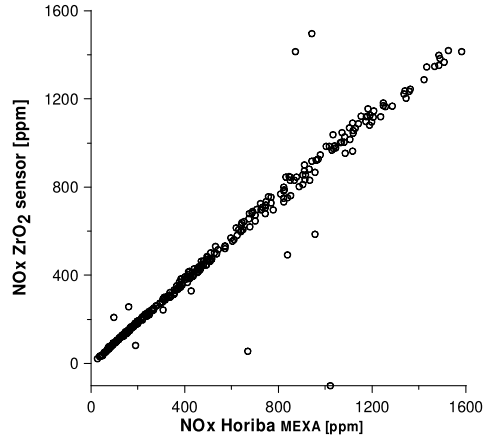


Figure 2: Chemiluminiscence vs sensor 1  $ZrO_2$  sensor measurements for the steady dataset.

As a preliminary step, the static calibration of the zirconia sensors was performed using the Horiba MEXA chemiluminiscence system as calibration standard. The important dependability of the exhaust gas  $NO_x$  concentration when varying the engine operating conditions was profited for the steady calibration. The dataset consisted of 353 independent tests, where engine speed, injected fuel quantity and EGR rate were varied, causing  $NO_x$  concentration variations to cover the sensor measuring range. Figure 2 illustrates steady results (only for sensor 1). After the elimination of the outliers (usually caused by errors in the measurement procedure or in the human operation of the calibration standard) using the box and whiskers method, a linear fit was performed. Mean absolute resulted 2.05%, and residuum standard deviation 1.61%. This was judged to be a quite good result.

#### 3.1. Methodology for dynamic calibration

The second step in the calibration procedure consisted in the identification of the sensor dynamics. A well-known method consists of using a step transition in the measured quantity[20].

However, usual means for providing step-like transition in gas concentration are complex set-ups[13]. The method presented in the present paper is based on the variation of the SOI, which can be easily done in current engines during their normal operation. In order to decouple as much as possible the effect of SOI variations on the air path of the engine, EGR rate was set to zero (EGR valve fully closed) during the tests.

Although other variables could be used for affecting the  $NO_x$  concentration (e.g. EGR valve control), SOI was selected because:

- SOI varies the exhaust gas composition in an important way, producing  $NO_x$  concentration variations.
- SOI variations produce low variations for turbine intake temperature and pressure. Hence, conditions at the turbine inlet are not importantly varied, and the turbocharged speed and boost pressure are not significantly affected; since the EGR valve was closed, the effect of the slight variation in the exhaust pressure was neglected. This was considered as a key factor since pressure and temperature variations are associated with slow transients (because of mass and heat accumulation) which would affect the  $NO_x$  concentration.
- Other control variables correspond to slow acting valves, which will distort the step-like profile in the gas composition. However, the system response to SOI variation can be considered instantaneous: SOI is electronically applied, thus no actuation delay is expected beyond the cycle-to-cycle response time (and software delay). Additionally, since no exhaust gas recirculation was performed,  $NO_x$  concentration at the cylinder exhaust port is only dependent on the trapped air mass quantity and temperature, and injection settings during the previous cycle ( $NO_x$  contained in the residual gas fraction is reburned during the combustion[21]). Finally, gas transport delay from the cylinder to the  $ZrO_2$  sensor (located at least 1m from the exhaust port) is of a few tens of ms (considering typical velocities of the flow in the exhaust manifold downstream the turbine for the current engine exceeding 20 m/s).

For demonstrating the effect of sharp variations in SOI on the engine behaviour, 21 tests consisting in several consecutive steps were performed at different engine speeds (from 1000 to 3000rpm) totalling 105 unique step transitions with different initial  $NO_x$  concentrations (i.e. different initial engine operating conditions) and step sizes (ranging from 1° to 9° in SOI). Data was later used for the sensor dynamics identification.

As a characteristic example of the tests, Figure 3 shows the evolution of  $NO_x$  measurements during a 2° step in SOI at 1000 rpm and 20 mg/stroke of fuel, while Figure 4 illustrates that other significant variables (as boost and exhaust pressure, gas temperatures, coolant temperature and air mass flow) do not vary in an important way during the tests. The maximum variation in these properties was 2.8% for exhaust pressure (considering a moving average filtered value), while the rest of them varied less than 0.5%.

#### 4. Application example to several $NO_x$ sensors

For illustrating the applicability of using data derived from SOI steps, a simple dynamic identification was done assuming a linear first order model behaviour (other possible model structures with physical insight could be found in [22]). The generic step response of a first order system can be modelled through the equation (1),

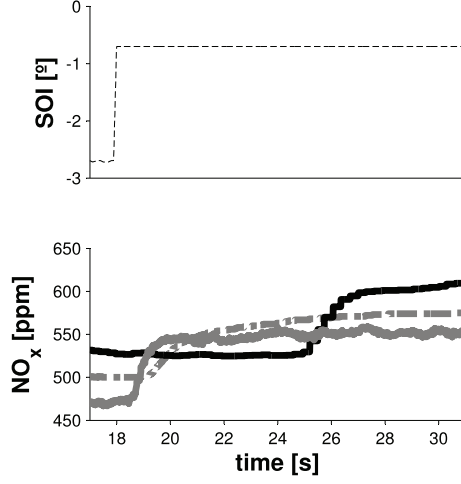


Figure 3: Measured evolution of  $NO_x$  concentration during a SOI step, sensor 1 is represented in dashed grey, sensor 2 in solid grey, and HORIBA MEXA-7100 in solid black.

$$\begin{aligned} NO_x &= a + G \left(1 - e^{-\frac{t-\tau}{k}}\right) & t \geq \tau \\ NO_x &= a & t < \tau \end{aligned} \quad (1)$$

where  $a$  is the  $NO_x$  initial value before the step,  $G$  is the step-amplitude,  $t$  the time. Sensor delay  $\tau$  represents the delay from the application of SOI (judged to be instantaneous) and the start of the sensor output variation, and  $k$  stands for the sensor time constant. Center plot in Figure 5 clarifies the interpretation of  $\tau$  and  $k$ .

For each individual step and sensor,  $k$  and  $\tau$  were obtained. For the coefficient identification, a least-square fit of equation (1) was performed (although more robust recursive identification techniques could be used for the online case[23]). Figure 5 illustrates an example of the fit obtained for sensor 1 (top), sensor 2 (center) and the gas analyzer(bottom).

Average values of the identified delay  $\tau$  and time constant  $k$  and their deviations are shown in Table 2. As expected,  $ZrO_2$  sensors delay ( $\tau$ ) was lower than chemiluminescence system delay: mainly caused by the treatment operations of Horiba MEXA 7100DEGR as long as transport delay in the long gas line feeding the measurement system (12 m) also adds a non-negligible delay due to the low flow quantity allowed[24]. In the case of the time constant, sensor 2 is faster than the other ones. The output of the different sensors is plotted in Figure 3, and it can be clearly noticed the significant lower delay for the  $ZrO_2$  sensors with respect to the gas analyser, in accordance with Table 2. On the other hand, the standard deviations obtained for  $k$  and  $\tau$  estimates merit for additional analysis, as they suggest that the sensor behaviour could be affected by the gas concentration conditions during the test.

No direct influence was found on the sensors response from gas speed, temperature or pressure, since the identified parameters do not vary significantly with these conditions (not shown). In order to analyse the effect of the initial  $NO_x$  concentration ( $NO_{x,0}$ ) and of the step size ( $\Delta NO_x$ ), scatter plots of  $k$  and  $\tau$  are presented in Figures 6 and 7 for the two  $ZrO_2$  sensors.

In the case of sensor 2, it seems that abnormal dynamic parameters are identified for smaller

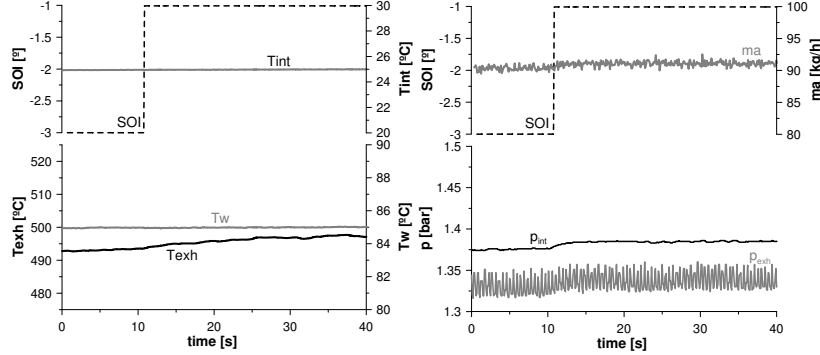


Figure 4: Coolant temperature ( $T_w$ ), exhaust manifold gas temperature ( $T_{exh}$ ), intake manifold air temperature ( $T_{int}$ ), exhaust manifold pressure ( $p_{exh}$ ), intake manifold pressure ( $p_{int}$ ) and air mass flow ( $m_a$ ) evolution during step-like test at 2000 rpm and 50 mg/stroke.

	Horiba	Sensor 1	Sensor 2
$k$ [s]	0.86	1.58	0.43
$\sigma_k$	0.74	1.06	0.41
$\tau$ [s]	7.35	0.87	0.50
$\sigma_\tau$ [s]	0.78	0.40	0.22

Table 2: Mean and standard deviations for the identified delay  $\tau$  and time constant  $k$ .

step sizes (below 75 ppm). The reason could be that in the case of small steps, the concentration profile is not step-like, but affected by other slower variations (temperature, pressure, etc.) that are not negligible in opposition to the assumption made in section 3. This explains the large deviations obtained in  $k$  and  $\tau$  as presented in Table 2. For larger step size, the identified  $\tau$  and  $k$  are quite constant, as shown in Table 3 where tests with  $\Delta NO_x < 75$  ppm have been removed.

	Horiba	Sensor 1	Sensor 2
$k$ [s]	0.78	1.10	0.37
$\sigma_k$	0.08	0.42	0.09
$\tau$ [s]	7.44	0.73	0.54
$\sigma_\tau$ [s]	0.18	0.22	0.17

Table 3: Identified dynamics for  $ZrO_2$  sensor considering tests with  $\Delta NO_x > 75$  ppm.

Note that only low  $\Delta NO_x$  could be applied in tests with low  $NO_{x,0}$ , because SOI actuation did not allowed significant variations in the gas concentration. Hence,  $NO_{x,0}$  and  $\Delta NO_x$  are correlated. This explains the effect of high deviation presented for low  $NO_{x,0}$  values shown in right-hand plots of Figures 6 and 7. On the other hand, in some tests with high  $NO_{x,0}$  ( $> 1800$  ppm), very small  $\Delta NO_x$  were applied ( $< 75$  ppm), which explains the large deviation presented in Figure 6 for high  $NO_{x,0}$  values.

In the case of sensor 1, the same effect for smaller steps is noticed; however, in this case the

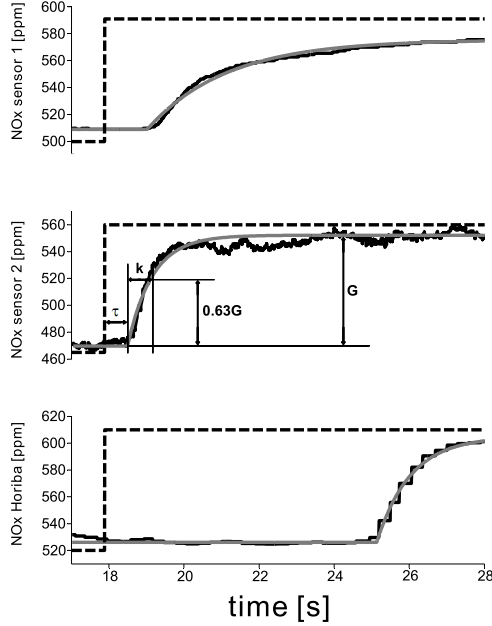


Figure 5: Top: Identified model (grey) and measured evolution (black) for the sensor 1; middle: Identified model (grey) and measured evolution (black) for the sensor 2 including a graphical interpretation of sensor delay ( $\tau$ ) and time constant ( $k$ ) is provided. Bottom: identified model and measured evolution for the chemiluminescence sensor 1.

identified parameters suggest that sensor response is faster ( $k$  tends to be smaller) when larger step size is applied. This effect was persistent during the tests and was not found in sensor 2 where  $k$  presents a smaller deviation, and it could be related to the different response profiles shown by the two sensors (as illustrated in Figure 3) and the limited capacity of the simple first order model to represent correctly the sensors response (which is represented in Figure 5).

Once tests with  $\Delta NO_x < 75$  ppm were removed, new values for  $\tau$  and  $k$  were obtained. As shown in Table 3, new deviations were significantly lower than those initially calculated, specially for the gas analyser and sensor 2. In the case of sensor 1, the deviation is still high because of the no constant behaviour of the identified dynamics, as justified in the previous paragraph. According to this experience, for the correct identification of sensor dynamics, minimum excitation step size of  $\pm 100$  ppm is advised. Depending on the operating conditions,  $2^\circ$  to  $3^\circ$  step in SOI can be sufficient; however, for low initial  $NO_x$  concentrations this could not be sufficient, and it is not advised using such operating conditions for the method (as significant variations in torque could be obtained).

Finally, one of the main problems of automotive sensors is their degradation during their lifespan. For ensuring the correct performance of the control structure, the system has to be capable of checking the sensor periodically. This methodology could be useful for these purposes. As an example, sensor 1 has been evaluated with data coming from the same sensor when in new condition (two years before the reported tests). 20 steps of SOI were used for the identification of the dynamics in new condition, and compared with the dynamics of the sensor once aged.



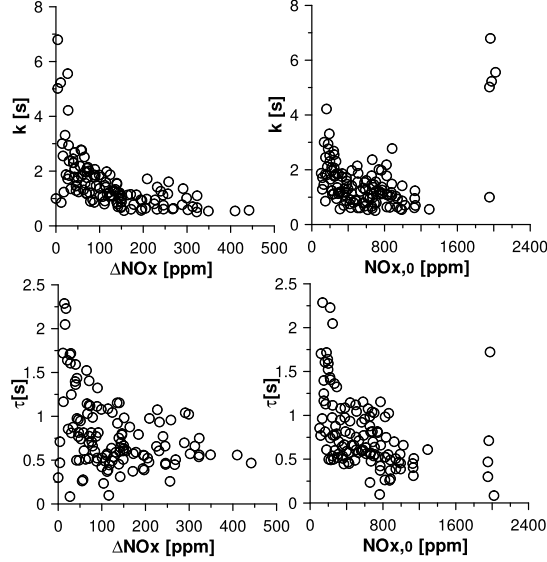


Figure 6: Time response  $k$  and delay  $\tau$  for the  $NO_x$  sensor 1 as function of the concentration step  $\Delta NO_x$  and the initial concentration  $NO_{x,0}$ .

As shown in Figure 8 and Table 4, the sensor response has not been significantly affected in the meantime, and it can be concluded that the sensor has maintained its dynamical performance.

	sensor 1 new cond.	sensor 1 aged cond.
$k$ [s]	1.08	1.10
$\sigma_k$	0.32	0.42

Table 4: Identified dynamics for  $ZrO_2$  sensor 1 considering tests with  $\Delta NO_x > 75 ppm$  for aged and new condition operation.

## 5. Perspective for on-board application

Presented method based on shifting SOI could be easily applied during operation phase of automotive diesel engines. That means that the ECU could use this test for identifying sensor dynamical response, and diagnosing sensor and system performance. This could be periodically done during specific conditions of the engine run.

Checking sensor dynamics could be used for sensor diagnostics, and also for updating the control structures. The knowledge of the dynamic sensor characteristics is needed for the application of model based predictive control concepts[25], and for data fusion and signal reconstruction techniques[7, 26, 27], which are being developed in automotive applications. For control application purposes, the dispersion of the sensor model can be corrected online using the combination of the mentioned techniques and the sensor measurements using the proposed method. In this way, the robustness of the control law can be checked regarding this dispersion.

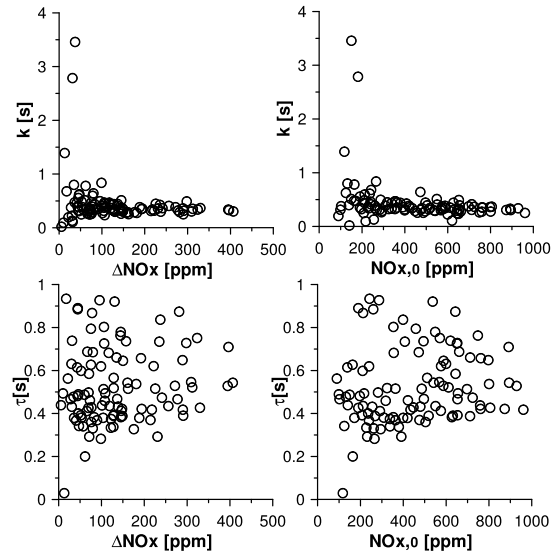


Figure 7: Time response  $k$  and delay  $\tau$  for the  $NO_x$  sensor 2 as function of the concentration step  $\Delta NO_x$  and the initial concentration  $NO_{x,0}$ .

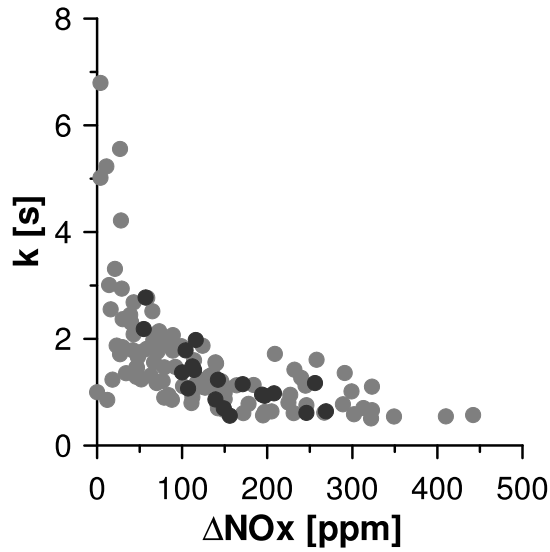


Figure 8: Time response  $k$  for the  $NO_x$  sensor 1 as a function of the concentration step  $\Delta NO_x$ . The sensor response in new condition is represented in black and once aged is represented in grey.

Note that presented results correspond to  $NO_x$  sensor located upstream the after-treatment de-

vices. Hence, the presented methodology will be of direct application for sensors in this position, which can be usually for feed-forward control of the SCR system[28]. For the most common case of sensor located downstream the SCR system, the following two aspects must be considered:

- The method will not be valid as far as the SCR is operating, mainly due to the important decreasing of the steady-state raw  $NO_x$  concentration (about 80%) and the cross sensitivity to ammonia affecting  $NO_x$  measurement[28]. Because of these, the dynamic characteristics of the signal can be importantly distorted (filtering the signal and thus losing the step-like behaviour). However, in this case the method could be still used for SCR system diagnosing, although further research would be needed.
- Even in the case the SCR is not operating, the possibility of exciting the downstream  $NO_x$  sensor needs to be checked: depending on the signal dynamics and the volume of after-treatment devices, the gas concentration can sufficiently keep its step-like profile[29]. This issue must be verified beforehand using for that two sensors, one upstream and the other downstream the after-treatment system, although once established the feasibility of the method, the first sensor can be removed. Finally,  $NH_3$  storage mechanism could also contribute to unexpected variations in the  $NO_x$  concentration at the SCR outlet, and hence, sufficient delay is needed between the SCR cut-off and the dynamic characterisation checking.

Excellent operating condition for performing these checks is highway operation (where torque and engine speed are reasonably constant during long periods). Figure 9 shows the variation in  $NO_x$  concentration and torque when SOI is varied in a 2-degree step profile while keeping constant injected mass flow and engine speed. As shown in the plot for extreme variations in SOI, raw  $NO_x$  production can be doubled with less than 10% impact on torque; that means that driveability can be ensured while the test is performed (corrections on injected fuel mass can be performed for maintaining the engine torque to its set-point causing the driver to be blind to the test). The increase in  $NO_x$  emission during the sensor testing should not importantly impact the overall emissions, since a few seconds are enough for the test (and also a descendent step could be used). On the other hand, in engines with SCR technology and  $NO_x$  sensor located upstream the SCR, the SCR could cope with the excess  $NO_x$ .

## 6. Conclusions

A simple on-engine experiment for  $NO_x$  sensor characterisation has been presented. The method uses the engine as a gas generator and the procedure consists of applying steps in SOI producing sharp variations in  $NO_x$  concentration. With a simple variation of 2-3° in SOI,  $NO_x$  concentration is varied whilst torque values and fluid conditions remain approximately constants.

This method allows the determination of the dynamic response of the sensor over its entire useful life and the detection of faults in the same. A simple mathematical modelling, taking as a reference a first order model response, has been proposed, although more complex identification techniques can be used. Due to its nature, on-board application could be used for sensor and system diagnosis. Also, the implementation of this kind of sensors in the control structure is a matter that is being studied currently, and this method could be useful to on-line dynamic calibration and development of adaptive models included in a predictive control structure.

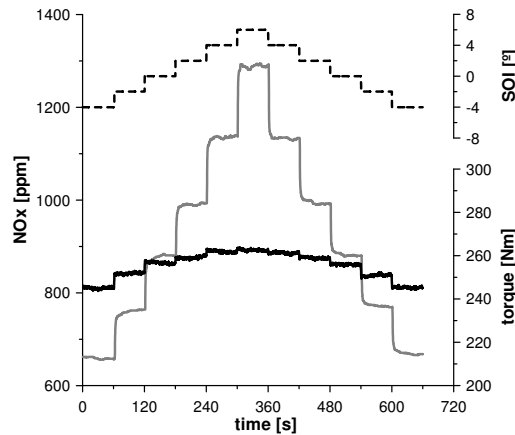


Figure 9:  $NO_x$  concentration measured by  $ZrO_2$  sensor 1 (grey) and torque evolution (black) at 2000 rpm and 50 mg/stroke when varying SOI (dashed black).

## Acknowledgement

The authors thanks R. Luján and G. Couture for their valuable contribution in the experimental part of the present work. This work has been partially supported by Ministerio de Ciencia y Tecnología through Project PLANUCO No.TRA2006-15620-C02-02.

- [1] 2007 Regulation (EC) No 715/2007 of the European Parliament and of the Council of 20 June 2007 on type approval of motor vehicles with respect to emissions from light passenger and commercial vehicles (Euro 5 and Euro 6) and on access to vehicle repair and maintenance information. *Official Journal of the European Union* **L171**.
- [2] Broatch A, Luján JM, Serrano JR and Pla B 2008 A procedure to reduce pollutant gases from Diesel combustion during European MVEG-A cycle by using electrical intake air-heaters. *Fuel* **87(12)** 2760-2778.
- [3] Kato N, Nakagaki K and Ina N. 1996 Thick Film  $ZrO_2$   $NO_x$  Sensor *SAE paper* 960334.
- [4] Hafner M, Schüler M, Nelles O and Isermann R 2000 Fast neural networks for diesel engine control design. *Cont. Eng. Pract.* **8** 1211-1221.
- [5] Arregle J, López JJ, Guardiola C and Monin C 2010 On Board  $NO_x$  Prediction in Diesel Engines: A Physical Approach. *Automotive Model Predictive Control: Models, Methods and Applications, Del Re L et al. (Eds)* ISBN-1849960704, Springer.
- [6] Smith J. Demonstration of a fast response on-board  $NO_x$  sensor for heavy-duty diesel vehicles. July 2000. Final Report SwRI Project No. 03-02256 Contract No. 98-302. *Southwest Research Institute Engine and Vehicle Research Division*.
- [7] Manchur TB and Checkel MD 2005 Time Resolution Effects on Accuracy of Real-Time  $NO_x$  Emissions Measurements *SAE paper* 2005-01-0674.
- [8] Moos R 2005 A Brief Overview on Automotive Exhaust Gas Sensors Based on Electroceramics. *Int. J. Appl. Ceram. Technol.* **2** 401-413.
- [9] Riegel J, Neumann H and Wiedenmann H-M 2002 Exhaust gas sensors for automotive emission control. *Solid State Ionics* **152-153** 783-800.
- [10] Nieuwstadt MV and Upadhyay D 2005 Diagnosis of a urea SCR catalytic system. *US Patent* 6925796.
- [11] Kim Y-W and Nieuwstadt MV 2006 Threshold Monitoring of Urea SCR Systems. *SAE paper* 2006-01-3548.
- [12] Luján JM, Galindo J, Serrano JR and Pla B 2008 A methodology to identify the intake charge cylinder-to-cylinder distribution in turbocharged direct injection Diesel engines. *Meas. Sci. Technol.* **19** 065401.
- [13] Regitz S and Collings N 2008 Fast response air-to-fuel ratio measurements using a novel device based on a wide band lambda sensor. *Meas. Sci and Technol.* **19** 075201.
- [14] Tobias P, Martensson P, Göras A, Lundström I, Lloyd Spetz A 1999 Moving gas outlets for the evaluation of fast gas sensors *Sensors and Actuators B* **58** (1999) 389-393.

- [15] Galindo J, Luján JM, Climent H and Guardiola C 2007 Turbocharging System Design of a Sequentially Turbocharged Diesel Engine by Means of a Wave Action Model *SAE paper 2007-01-1564*.
- [16] Bermúdez V, Luján JM, Serrano JR and Pla B 2008 Transient particle emission measurement with optical techniques. *Meas. Sci. Technol.* **19** 065404.
- [17] Arregle J, Bermúdez V, Serrano JR and Fuentes E 2006 Procedure for engine transient cycle emissions testing in real time. *Exp. Thermal and Fluid Science* **30** 485-496.
- [18] Chan SH, Chen XS and Arcoumanis C 1997 Measurement and signal reconstruction of transient nitric oxide emissions in the exhaust of a turbocharged diesel engine *Trans. ASME, J. Dynamic Systems, Measmt Control* **119** 620-630.
- [19] Geivanidis S and Samaras Z 2008 Development of a dynamic model for the reconstruction of tailpipe emissions from measurements on a constant volume sampling dilution system. *Meas. Sci and Technol.* **19** 015404
- [20] Ogata K 2001 *Modern Control Engineering* (4th Edition), Prentice Hall.
- [21] Arregle J, Lopez J and Mocholi E 2005 Diesel  $NO_x$  Modeling with High Initial  $NO_x$  from EGR or Re-Entrained Burned Gases *SAE paper 2008-01-1188*
- [22] Zhuiykov S 2008 *Electrochemistry of Zirconia Gas Sensors Taylor & Francis Group, LLC*
- [23] Ljung L 1999 *System Identification: Theory for the User*, Prentice Hall PTR, Upper Saddle River, NJ.
- [24] Horiba MEXA-7100DEGR Instruction Manual, HORIBA, August 2001
- [25] Luján JM, Climent H, Guardiola C and García-Ortiz JV 2007 A comparison of different algorithms for boost pressure control in a heavy-duty turbocharged diesel engine. *Proc. Inst. Mech. Eng. Part D: Jour. Automob. Eng.* **221** 629-640.
- [26] Kalman RE 1960 A New Approach to Linear Filtering and Prediction Problems. *Journal of Basic Engineering* **82**(1) 35-45.
- [27] Alberer D, del Re L 2009 Fast Oxygen Based Transient Diesel Engine Operation. *SAE paper 2009-01-0622*
- [28] Hofmann L, Rusch K and Fischer S 2004 Onboard Emissions Monitoring on a HD Truck with an SCR System Using  $NO_x$  Sensors. *SAE paper 2004-01-1290*
- [29] Keefe G and Mueller R 2001 Experience with SCR Technology for Diesel Exhaust Emission Control of Trucks in ASIA, Europe and North America. *AVECC Bangkok*.